

EVOLUTIONARY SEQUENCES OF STELLAR MODELS OF INTERMEDIATE AND HIGH MASS INCLUDING CONVECTIVE CORE OVERSHOOTING

CHAO-WEN CHIN AND RICHARD B. STOTHERS

Institute for Space Studies, NASA/Goddard Space Flight Center, 2880 Broadway, New York, NY 10025

Received 1991 January 14; accepted 1991 March 26

ABSTRACT

Stellar evolution with parameterized overshooting from the convective core has been studied for the stellar mass range $M/M_{\odot} = 3\text{--}30$ and for the initial chemical composition range $X_e = 0.650\text{--}0.739$ (hydrogen) and $Z_e = 0.021\text{--}0.044$ (metals). Evolutionary sequences run from the zero-age main sequence to the end of core helium burning, but emphasis is placed here on the core helium-burning phase. Convective core overshooting during the previous main-sequence phase leads, in most cases, to a shortening of the blue loop on the H-R diagram that forms when helium is being depleted in the core. On the other hand, convective overshooting from the helium-burning core has the opposite effect. A larger initial metals abundance also tends to shorten the blue loop. In an extreme case the blue loop can be fully suppressed, but in a marginal case the normal trend can be reversed. The fraction of the core helium-burning lifetime that is spent in the blue phase is generally very sensitive to the physical input parameters. Detailed tables and plots of evolutionary tracks on the H-R diagram are provided.

Subject headings: stars: evolution — stars: interiors — stars: massive

1. INTRODUCTION

The case for a significant amount of convective overshooting from the convective core inside a star has been presented many times both theoretically and observationally, but the results so far have been contradictory (for a recent review see Wheeler 1990). The facts that are unarguably known concern only the basic theory. During the core hydrogen-burning phase, a star acquires a larger helium core, a brighter luminosity, and a longer lifetime than in the absence of overshooting (Stothers 1970). If overshooting is so extensive that the star possesses only a thin original-composition envelope, the effective temperature is increased. But if overshooting is either slight or moderate, the effective temperature is reduced (Stothers 1972; Prather & Demarque 1974; Maeder 1974); in an extreme case, a very massive star may even cross the whole H-R diagram before central hydrogen exhaustion (Masseevitch et al. 1979). During the core helium-burning phase, the luminosity is brighter, the lifetime is shorter, and the blue loop that emerges from the region of red supergiants on the H-R diagram is less extended and rises less steeply than in the absence of overshooting (Matraka, Wassermann, & Weigert 1982; Becker & Cox 1982). Much recent work, cited below, has supported these basic conclusions, but only as long as mass loss is unimportant.

In the interest of testing further these conclusions that have already been reached for the core helium-burning phase, on the supposition that they might still be vulnerable, we have constructed a large grid of over 100 evolutionary sequences for stars of moderate to high mass, while ignoring both the lowest and highest masses where stellar wind mass loss is probably important for the post-main-sequence evolution. Our results for the characteristics of the blue loops significantly confirm and extend the earlier results, but they also contradict them in certain situations, which should serve as a salutary reminder of how fragile the blue loops really are.

2. INPUT PHYSICS AND MODEL ASSUMPTIONS

To have a useful comparison with our previously published evolutionary sequences, we have adopted the same input physics as described elsewhere (Stothers & Chin 1973). Nuclear reaction rates are unchanged, except that the uncertainty in the $^{12}\text{C}(\alpha, \gamma)^{16}\text{O}$ reaction rate is now represented by the multiplicative constant θ_{α}^2 , which originally meant the reduced α -particle width of the 7.12 MeV level in ^{16}O but is used here to subsume all the other uncertainties as well. The standard reaction rate given by Fowler, Caughlan, & Zimmerman (1975) is thus represented approximately with $\theta_{\alpha}^2 = 0.05$, but most of the new experimental results, as reviewed by Maeder (1990), suggest a rate 3–5 times higher. Therefore, we adopt (as before) $\theta_{\alpha}^2 = 0.1$, which is probably accurate to within a factor of 2 for the main phase of core helium burning in our stellar models.

Cox-Stewart opacities are adopted, also as before. In the outer convection zone, the ratio of convective mixing length to local pressure scale height is taken to be $\alpha_P = 1$, unless otherwise noted. Two initial hydrogen abundances by mass, $X_e = 0.739$ and 0.650 , and two initial metals abundances by mass, $Z_e = 0.021$ and 0.044 , are used, because these four values bracket the likely ranges of Population I chemical composition in our region of the Galaxy. Stellar masses of $3, 5, 7, 10, 15$, and $30 M_{\odot}$ are chosen to represent the mass range under present consideration.

Convective core overshooting is parameterized by a quantity d/H_P , representing the ratio of the overshoot distance beyond the classical Schwarzschild core boundary (where $\nabla_{\text{ad}} = \nabla_{\text{rad}}$) to the local pressure scale height. In the overshoot region, chemical mixing is assumed to be complete, while the temperature gradient is taken to be the adiabatic one. In the case of evolved stellar models, only the first assumption is important for the star's overall structure and observable properties. In the absence of more definite knowledge and in the heuristic spirit of the present study, we take d/H_P to be a con-

stant for each stellar mass and for each of the two primary phases of stellar evolution. We differentiate main-sequence evolution from post-main-sequence evolution. For reasons of economy, three cases are considered here: (1) no overshooting during both evolutionary phases; (2) overshooting only during the main-sequence phase; and (3) overshooting during both phases, under the assumption of the same value of d/H_P for each phase. (The reasons for case 2 will be explained below.) Following our two earlier studies of the main-sequence phase (Stothers & Chin 1981, 1985), we adopt $d/H_P = 0, 0.35$, and 0.70.

One complication that greatly affects the study of evolution without convective core overshooting is reduced, or even eliminated, when overshooting is significant. This is the problem of convective instability in the intermediate layers that lie between the homogeneous convective core and the homogeneous outer envelope. On the main sequence, the instability develops in stars more massive than $\sim 9 M_\odot$ and is usually handled by assuming semiconvection in the unstable layers. Shortly after the stage of central hydrogen exhaustion, the convective instability intensifies, this time above the hydrogen-burning shell, and leads to the development of a local semiconvective, or even fully convective, intermediate zone. Although such a zone exerts little influence on the evolution of stars less massive than $\sim 10 M_\odot$, it can be present even for stellar masses as low as $7 M_\odot$. During the phase of core helium depletion in stars of all masses, but with increasing importance at the smaller masses, convective instability breaks out again just beyond the formal convective core boundary. Computationally, it is usually either ignored or treated by assuming that a semiconvective zone develops. Toward the end of the phase of core helium burning, the instability may recur in outward-directed surges of full core convection (known as "helium spikes" or "breathing pulses"). Since the expanding helium-burning convective core must overcome a growing mean molecular weight barrier (heavier material being transported upward into lighter material), the extent of convective overshooting is uncertain and may be much smaller than in the case of the constantly receding hydrogen-burning convective core.

Since convective core overshooting with $d/H_P > 0.35$ eliminates these convective instabilities in nearly all layers of the intermediate zones, we will usually be justified here in completely ignoring convection in those regions. For the purposes of comparison and interpolation, our present sequences with $d/H_P = 0$ have also been computed by making the same simplifications.

3. EVOLUTION ON THE HERTZSPRUNG-RUSSELL DIAGRAM

Evolutionary tracks on the H-R diagram, running from the zero-age main sequence to a stopping point close to the end of core helium burning ($Y_c = 0.03$), are displayed for our new models in Figures 1–10. The tracks shown include all the cases calculated in our main parameter grid, except for cases 2 and 3 with $Z_e = 0.044$. Tracks plotted as dashed lines displayed no blue loops in the original calculations. However, we found that blue loops could be induced by allowing downward convective overshooting from the outer convection zone (Stothers & Chin 1991). Choosing downward overshoot distances $D \approx 0.4H_P - 0.7H_P$, which are by no means implausible in view of existing

uncertainties about envelope convection, led to perturbed evolutionary tracks that fitted the overall pattern of other tracks better. Therefore, we adopted them. They are clearly differentiated from all of the tracks that are displayed without blue loops, because in the latter tracks blue loops could only be triggered by assuming $D > 1.5H_P$. On the other hand, there are unrelated ways to trigger blue loops (§ 4).

The effect of convective core overshooting is considerably more complex than that of convective envelope overshooting. Since core overshooting on the main sequence increases the helium core mass, the lifetime of the subsequent core helium-burning phase is shortened in comparison with the corresponding lifetime in the standard case. As a consequence, the hydrogen-burning shell does not burn outward as far, and therefore may not come sufficiently close to the hydrogen jump that defines the deepest penetration of the outer convection zone as to produce a high effective temperature along the blue loop. The upshot of this chain of events is that convective core overshooting on the main sequence normally shortens the length of the subsequent blue loop, a result that has already been obtained in comparable earlier studies.

Thus, with approximately the same input values of stellar mass, initial chemical composition, and effective $d/H_P \approx 0.35$, our models for $10 M_\odot$ agree well with those of Becker & Cox (1982) for $9 M_\odot$. Our models for 5 and $7 M_\odot$, however, are considerably less sensitive to d/H_P (if $d/H_P \leq 0.35$) than the models calculated by Matraka, Wassermann, & Weigert (1982) and by Huang & Weigert (1983); but those authors adopted an initial chemical composition, $(X_e, Z_e) = (0.602, 0.044)$, that is outside our chosen range. Even though the initial chemical compositions used by Bertelli et al. (1986) and Maeder & Meynet (1988) are similar to ours, their models for 5 and $7 M_\odot$ with $d/H_P \approx 0.3$ occupy somewhat shorter blue loops—yet not beyond what might be expected from the differences in the other input physics employed.

Four useful *new* results have emerged from the present calculations. First of all, if the overshoot distance during the main-sequence phase of evolution is increased still further, the blue loop can eventually become completely suppressed.

Second, a larger initial metals abundance enables convective core overshooting to suppress the blue loop more easily. Since a sufficiently large value of Z_e has a tendency to shrink the blue loop even in the absence of overshooting, the new results are easily understandable. Conversely, a small value like $Z_e = 0.021$ can require extremely large overshoot distances to suppress the blue loop (Fig. 11). The initial hydrogen abundance, on the other hand, is a mostly neutral factor in forming blue loops, unless it falls outside our chosen range (as in the calculations of Matraka et al. 1982 and Huang & Weigert 1983).

Third, convective core overshooting during the phase of core helium burning draws additional helium down into the convective core and so slightly prolongs the lifetime of this phase as compared with the case of a nonovershooting convective core. Consequently, the hydrogen-burning shell moves out slightly further, leading to a longer blue loop in case 3 than in case 2. However, the *luminosity* of the blue loop is hardly affected. Qualitatively similar results were previously obtained by Robertson (1971) and by Robertson & Faulkner (1972), who treated overshooting from the helium-burning convective core as a semiconvective process.

Fourth, whenever the occurrence of the blue loop is a marginal event, as in the case of stars of $5\text{--}15 M_{\odot}$ with an initial composition of $(X_e, Z_e) = (0.739, 0.021)$, relatively small perturbations can upset some of the above expectations. For example, at 5 and $7 M_{\odot}$ convective core overshooting with $d/H_P = 0.35$ leads to a normal blue loop, whereas the classical case produces no blue loop—unless the models are modified in some way, such as by imposing a small amount of downward convective overshooting from the outer convection zone.

Both the helium core mass and the mass of its convective central region are clearly critical factors in governing the size of the blue loop. These two quantities are plotted, in units of the star's total mass, as a function of stellar mass in Figure 12.

4. FURTHER TESTS

Except in marginal situations where the blue loop ends either inside or near the secularly unstable “yellow” region of the H-R diagram, the blue loop’s position (but *not* its duration) seems to be relatively robust for a fixed value of d/H_P . Since the evolutionary tracks that are most prone to forming blue loops are those with $(X_e, Z_e) = (0.650, 0.021)$, we have used this initial chemical composition for most of our additional sensitivity studies.

First, we varied α_p in the outer convection zone within the physically realistic range $0.5 \leq \alpha_p \leq 2.0$. When a blue loop developed (and in some cases of small and moderate α_p it did not), the maximum effective temperature attained was found to be only a weak function of α_p . This result fully conforms to the outcome of earlier studies (Lauterborn, Refsdal, & Roth 1971; Stothers & Chin 1973; Matraka et al. 1982; Huang & Weigert 1983).

Second, an increase of θ_{α}^2 by a factor of 10 in the $^{12}\text{C}(\alpha, \gamma)^{16}\text{O}$ reaction rate raised the maximum effective temperature attained on the blue loop by only a relatively small amount. Again, this agrees in a qualitative sense with earlier results (Iben 1966, 1972; Stothers & Chin 1973; Bertelli, Bressan, & Chiosi 1985; Brunish & Becker 1990).

A useful example from our present series of tests is given here for the blue loop at $15 M_{\odot}$ in case 3 with $d/H_P = 0.35$. With standard values of $\alpha_p = 1$ and $\theta_{\alpha}^2 = 0.1$, a blue loop did not develop. With $\alpha_p = 2$, however, a loop formed, reaching $\log T_e = 3.965$ and $\log(L/L_{\odot}) = 5.003$ at the blue tip. Or with $\theta_{\alpha}^2 = 1$ a loop also appeared, attaining $\log T_e = 4.059$ and $\log(L/L_{\odot}) = 5.008$. The difference in location of the blue tip is quite small.

Last, we considered the possibility of stellar wind mass loss. All of our computed tracks at $30 M_{\odot}$ can actually only be considered useful for interpolation purposes, owing to the large physical uncertainties arising from the probability of heavy mass loss in the red supergiant stages as well as from the probable presence of large-scale convection in the intermediate region above the hydrogen-burning layers. For initial masses of $3\text{--}15 M_{\odot}$, however, we have adopted an empirical formula for the rate of mass loss that was fitted by Nieuwenhuijzen & de Jager (1990) to observations of stars of all spectral types and luminosity classes. Mass loss as an influence on the blue tip turned out to be relatively unimportant in our test sequences that included it, just as other authors recently found for these more moderate initial masses (Bertelli, Bressan, &

Chiosi 1985; Doom, De Grève, & de Loore 1986; Maeder & Meynet 1987, 1988, 1989; Langer, Arcoragi, & Arnould 1989; Li & Huang 1990; Maeder 1990).

5. TABLES OF EVOLUTIONARY SEQUENCES

Summaries of the main numerical results in our cases 1, 2, and 3 are presented in Tables 1–4 for all six stellar masses and for all four initial chemical compositions. Convective core overshooting in cases 2 and 3 was calculated with $d/H_P = 0.70$.

Table 1 lists τ_H , the lifetime of core hydrogen burning, and τ_{He}/τ_H , the ratio of the lifetimes of core helium burning and core hydrogen burning.

Table 2 lists τ_b/τ_r , the ratio of the blue supergiant and red supergiant lifetimes during core helium depletion; the dividing line in effective temperature is taken, somewhat arbitrarily, at $\log T_e = 3.61$.

Table 3 lists $\log T_e$, the logarithm of the effective temperature, and $\log(L/L_{\odot})$, the logarithm of the luminosity, at the tip of the blue loop during core helium depletion.

Table 4 lists two entries for $\log(L/L_{\odot})$, the logarithm of the highest luminosity and the logarithm of the lowest luminosity on the red supergiant branch during core helium depletion; the rapid core-contraction stages preceding the arrival at the top of the red branch are not counted.

An additional table, Table 5, contains the equivalent summary of results for case 3 with $d/H_P = 0.35$.

Tables 6 and 7 list $\log(L/L_{\odot})$ and $\log T_e$ on the zero-age main sequence and on the terminal-age main sequence (located approximately at $X_c = 0.04$) for all cases.

To provide more details about the evolutionary sequences summarized in the first four tables, Tables 8–13 present selected models for the sequences based on our standard mixture $(X_e, Z_e) = (0.739, 0.021)$. These details may be compared with analogous ones that we published previously for evolution in stars of $10\text{--}120 M_{\odot}$, in which semiconvection and full convection in the intermediate zones were taken into account (Chin & Stothers 1990). In all of the tables, units of density and temperature are g cm^{-3} and K, respectively. Important stellar mass fractions are also tabulated: q_{core} , q_{shell} , and q_{env} , indicating the convective core boundary (including the overshoot region), the hydrogen-burning shell peak, and the inner boundary of the outer convection zone (tabulated only if $q_{\text{env}} < 0.9$). All models at important turning points and at significant acceleration and deceleration points on the H-R diagram are included among the various models tabulated. Note that main-sequence models for 10 , 15 , and $30 M_{\odot}$ with $d/H_P = 0.70$ were previously published in our 1990 paper; small differences between the new and the old models merely reflect minor differences in the choices of mass zoning and time steps.

A supplementary table, Table 14, compares the widely differing possible blue-to-red ratios of lifetimes during core helium depletion for pairs of sequences selected from our basic sequences and from our test sequences of § 4.

6. CONCLUSION

The present grid of evolutionary sequences with allowance for convective core overshooting should be useful for comparative studies of stellar evolution when the mass lies between 3

M_{\odot} and somewhat less than $30 M_{\odot}$, over most of the range of Galactic Population I chemical compositions. Of special interest are the blueward excursions of the evolutionary tracks on the H-R diagram during the core helium-burning phase. Convective core overshooting during the main-sequence phase normally leads to a reduction in the length of these blue loops, whereas convective core overshooting during the core helium-burning phase itself has the opposite effect. A larger value of the initial metals abundance also tends to diminish the blue loop. In an extreme case the blue loop can be completely suppressed, but in a marginal situation the normal trend can be reversed. In the latter case, a small amount of downward convective overshooting from the outer convection zone can, in some cases, trigger a blue loop. The duration of the blue loop is generally found to be very sensitive to the choices of physical input parameters.

Evolutionary sequences with main-sequence convective

core overshooting that have been published by other authors for initial masses $M_i \geq 3 M_{\odot}$ are listed in Table 15. With a few exceptions, the amount of overshooting was not parameterized in the same way as in our study, but it can be usually be represented approximately by an equivalent value of d/H_P , which is listed in the table. Notice that, in some sequences, the initial masses run up to $\sim 120 M_{\odot}$, stellar wind mass loss was included, and post-main-sequence evolution was also calculated. Three investigations used $Z_e < 0.02$ (Bertelli et al. 1986, 1990; Maeder 1990).

In a subsequent paper, the new evolutionary sequences, along with previous results, will be used to estimate upper and lower limits on d/H_P through a detailed comparison of the computed tracks with observed stars in the H-R diagram. It will be shown that the observations are consistent with $d/H_P = 0$ and that a relatively firm upper limit of $d/H_P \leq 0.2$ can be set by using post-main-sequence stars.

REFERENCES

- Becker, S. A., & Cox, A. N. 1982, *ApJ*, 260, 707
 Bertelli, G., Betto, R., Bressan, A., Chiosi, C., Nasi, E., & Vallenari, A. 1990, *A&AS*, 85, 845
 Bertelli, G., Bressan, A. G., & Chiosi, C. 1984, *A&A*, 130, 279
 ———. 1985, *A&A*, 150, 33
 Bertelli, G., Bressan, A. G., Chiosi, C., & Angerer, K. 1986, *A&AS*, 66, 191
 Bressan, A. G., Bertelli, G., & Chiosi, C. 1981, *A&A*, 102, 25
 Brunish, W. M., & Becker, S. A. 1990, *ApJ*, 351, 258
 Chin, C.-w., & Stothers, R. B. 1990, *ApJS*, 73, 821
 Cloutman, L. D. 1987, *ApJ*, 313, 699
 Cloutman, L. D., & Whitaker, R. W. 1980, *ApJ*, 237, 900
 de Loore, C. 1982, in IAU Symposium 99, Wolf-Rayet Stars: Observations, Physics, Evolution, ed. C. W. H. de Loore & A. J. Willis (Dordrecht: Reidel), 343
 Doom, C. 1982a, *A&A*, 116, 303
 ———. 1982b, *A&A*, 116, 308
 ———. 1985, *A&A*, 142, 143
 Doom, C., De Grève, J. P., & de Loore, C. 1986, *ApJ*, 303, 136
 Fowler, W. A., Caughlan, G. R., & Zimmerman, B. A. 1975, *ARA&A*, 13, 69
 Huang, R. Q., & Weigert, A. 1983, *A&A*, 127, 309
 Iben, I., Jr. 1966, *ApJ*, 143, 483
 ———. 1972, *ApJ*, 178, 433
 Langer, N., Arcoragi, J.-P., & Arnould, M. 1989, *A&A*, 210, 187
 Langer, N., & El Eid, M. F. 1986, *A&A*, 167, 265
 Lauterborn, D., Refsdal, S., & Roth, M. L. 1971, *A&A*, 13, 119
 Li, Y., & Huang, R. Q. 1990, *A&A*, 229, 469
 Maeder, A. 1974, in IAU Symposium 59, Stellar Instability and Evolution, ed. P. Ledoux, A. Noels, & A. W. Rodgers (Dordrecht: Reidel), 109
 Maeder, A. 1976, *A&A*, 47, 389
 ———. 1982, *A&A*, 105, 149
 ———. 1990, *A&AS*, 84, 139
 Maeder, A., & Mermilliod, J. C. 1981, *A&A*, 93, 136
 Maeder, A., & Meynet, G. 1987, *A&A*, 182, 243
 ———. 1988, *A&AS*, 76, 411
 ———. 1989, *A&A*, 210, 155
 Massevitch, A. G., Popova, E. I., Tutukov, A. V., & Yungelson, L. R. 1979, *Ap&SS*, 62, 451
 Matraka, B., Wassermann, C., & Weigert, A. 1982, *A&A*, 107, 283
 Nieuwenhuijzen, H., & de Jager, C. 1990, *A&A*, 231, 134
 Prantzos, N., Doom, C., Arnould, M., & de Loore, C. 1986, *ApJ*, 304, 695
 Prather, M. J., & Demarque, P. 1974, *ApJ*, 193, 109
 Pylyser, E., Doom, C., & de Loore, C. 1985, *A&A*, 148, 379
 Robertson, J. W. 1971, *ApJ*, 170, 353
 Robertson, J. W., & Faulkner, D. J. 1972, *ApJ*, 171, 309
 Staritsin, E. I. 1988, *Nauch. Inf.*, No. 65, p. 17
 Stothers, R. B. 1970, *MNRAS*, 151, 65
 ———. 1972, *ApJ*, 175, 431
 Stothers, R. B., & Chin, C.-w. 1973, *ApJ*, 179, 555
 ———. 1981, *ApJ*, 247, 1063
 ———. 1985, *ApJ*, 292, 222
 ———. 1991, *ApJ*, 374, 288
 Wheeler, J. C. 1990, in Supernovae, Sixth Jerusalem Winter School for Theoretical Physics, ed. J. C. Wheeler, T. Piran, & S. Weinberg (Singapore: World Scientific), 1
 Xiong, D. R. 1985, *A&A*, 150, 133
 ———. 1986, *A&A*, 167, 239

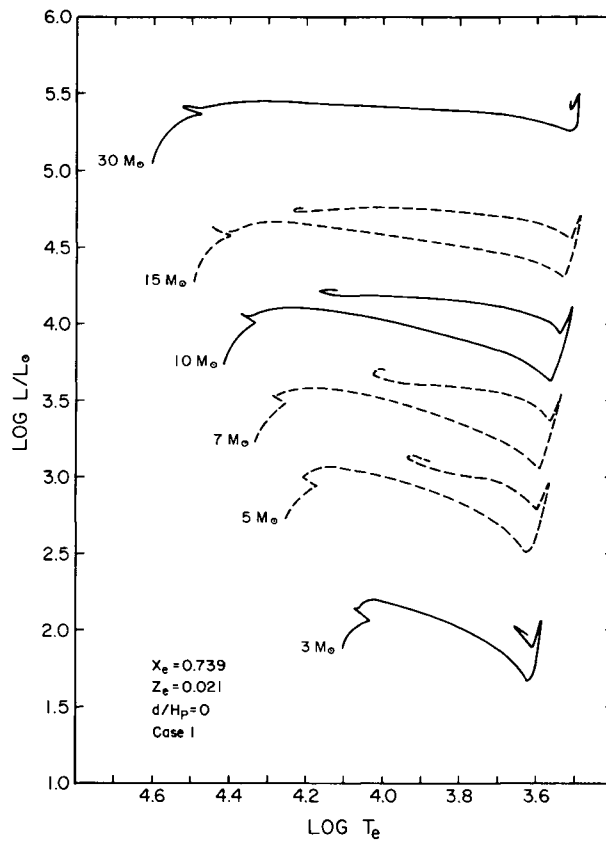


FIG. 1.—H-R diagram showing evolutionary tracks for case I with $X_e = 0.739$, $Z_e = 0.021$. Dashed tracks refer to our imposition of downward convective overshooting from the outer convection zone (otherwise, the blue loop does not occur).

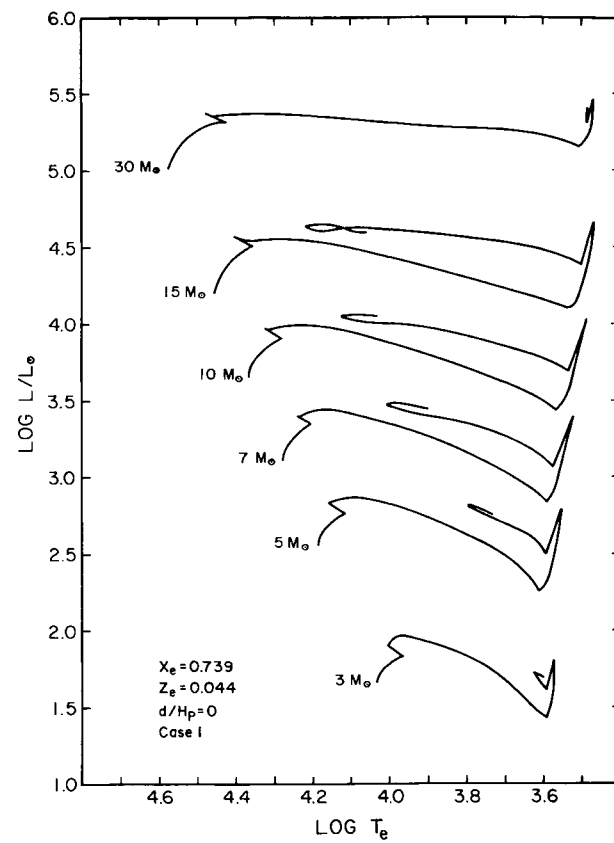


FIG. 2.—H-R diagram showing evolutionary tracks for case I with $X_e = 0.739$, $Z_e = 0.044$.

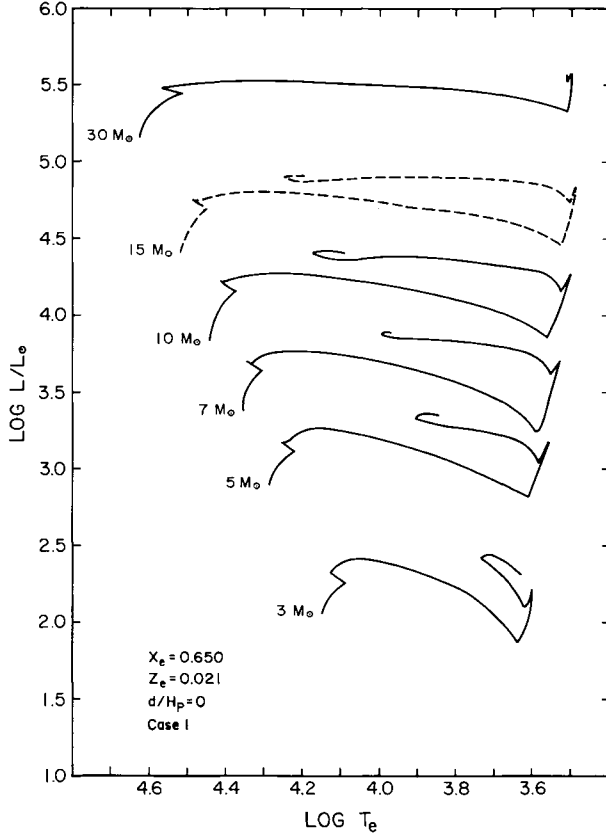


FIG. 3.—H-R diagram showing evolutionary tracks for case I with $X_e = 0.650$, $Z_e = 0.021$. The dashed track refers to our imposition of downward convective overshooting from the outer convection zone (otherwise, the blue loop does not occur).

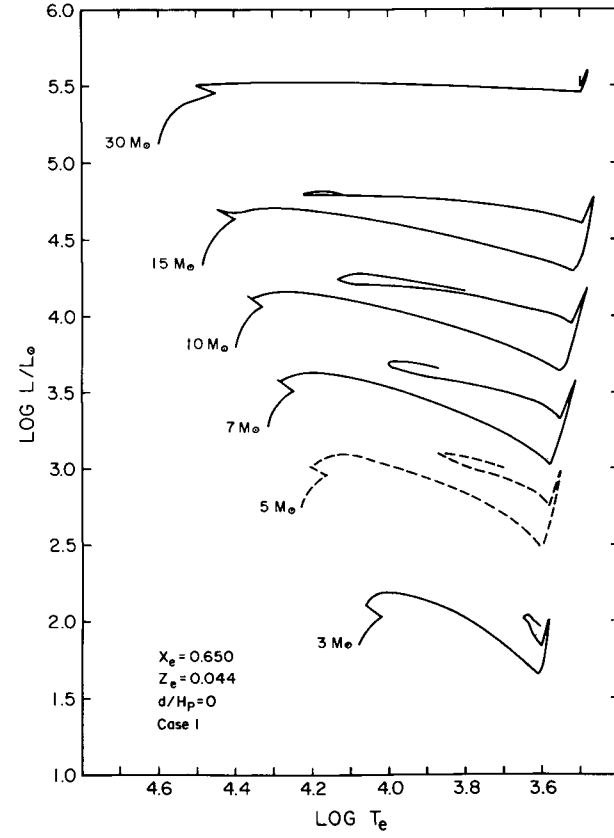


FIG. 4.—H-R diagram showing evolutionary tracks for case I with $X_e = 0.650$, $Z_e = 0.044$. The dashed track refers to our imposition of downward convective overshooting from the outer convection zone (otherwise, the blue loop does not occur).

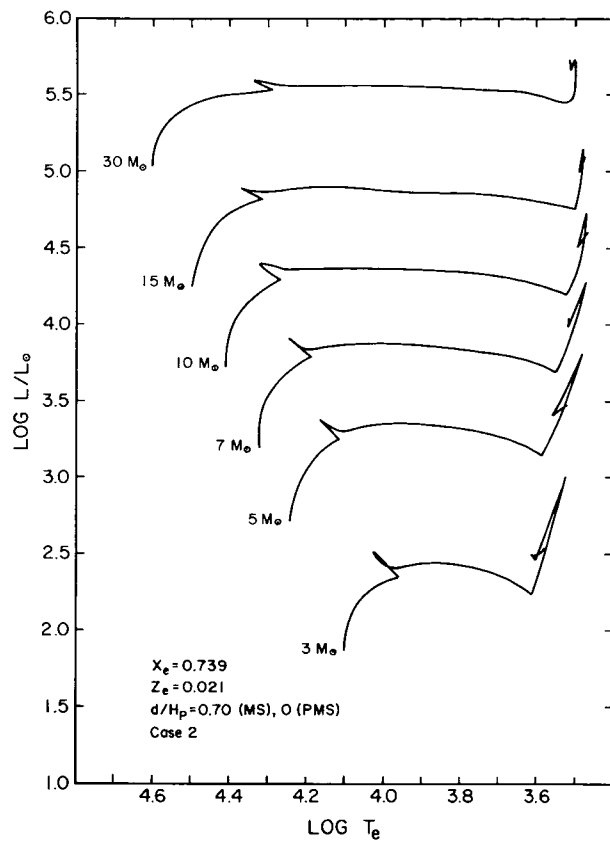


FIG. 5.—H-R diagram showing evolutionary tracks for case 2 with $X_e = 0.739$, $Z_e = 0.021$, and $d/H_P = 0.70$ (main sequence) and $d/H_P = 0$ (post-main sequence).

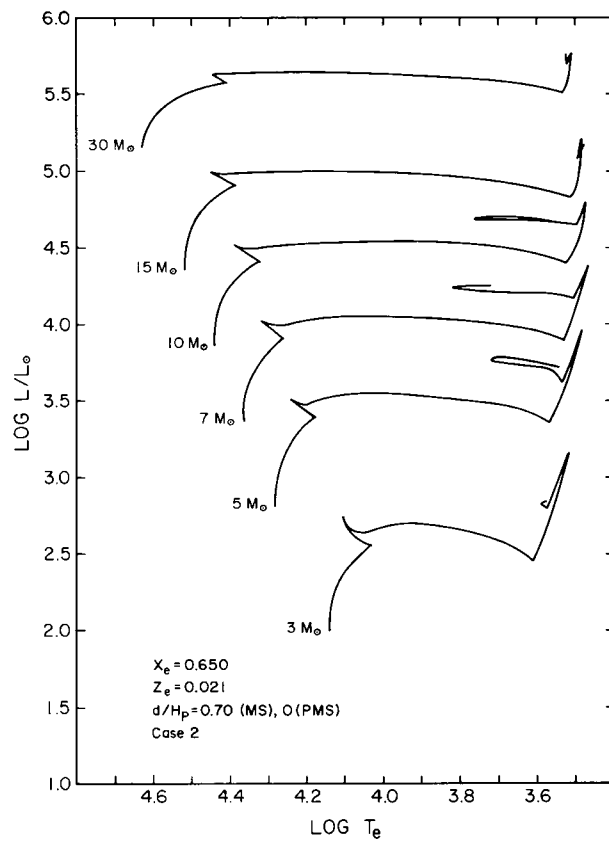


FIG. 6.—H-R diagram showing evolutionary tracks for case 2 with $X_e = 0.650$, $Z_e = 0.021$, and $d/H_P = 0.70$ (main sequence) and $d/H_P = 0$ (post-main sequence).

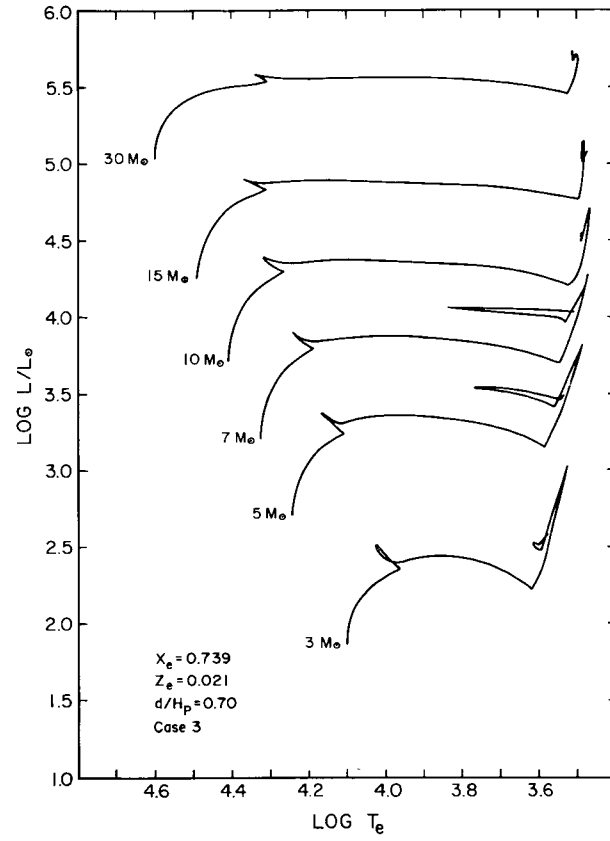


FIG. 7.—H-R diagram showing evolutionary tracks for case 3 with $X_e = 0.739$, $Z_e = 0.021$, and $d/H_P = 0.70$.

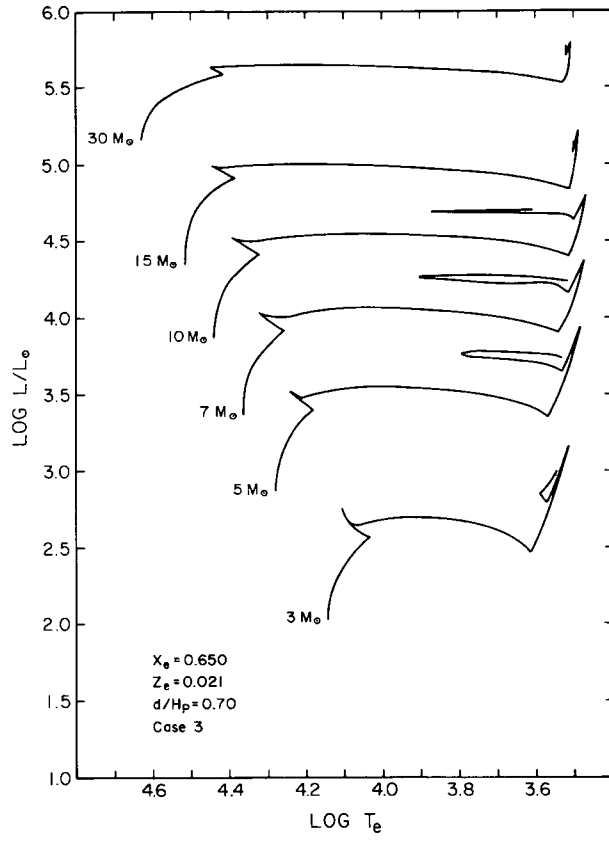


FIG. 8.—H-R diagram showing evolutionary tracks for case 3 with $X_e = 0.650$, $Z_e = 0.021$, and $d/H_P = 0.70$.

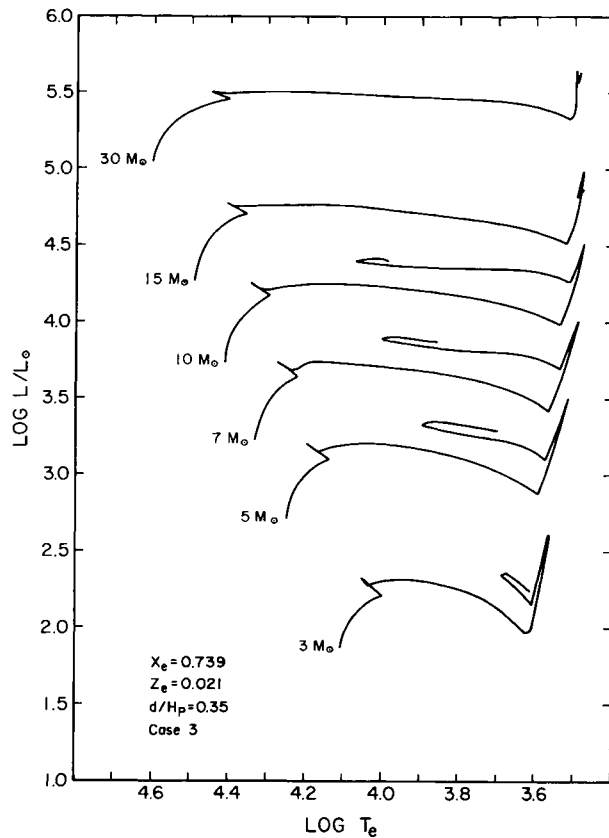


FIG. 9.—H-R diagram showing evolutionary tracks for case 3 with $X_e = 0.739$, $Z_e = 0.021$, and $d/H_P = 0.35$.

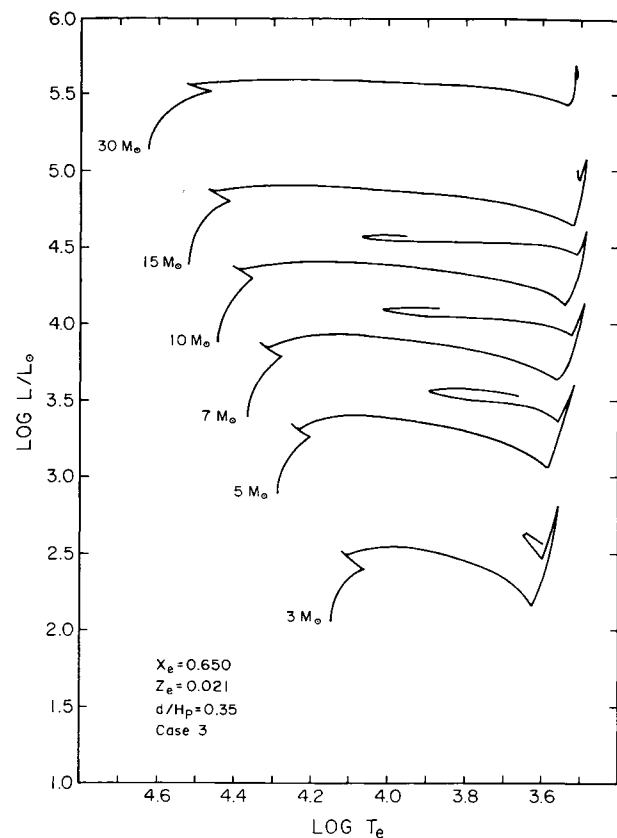


FIG. 10.—H-R diagram showing evolutionary tracks for case 3 with $X_e = 0.650$, $Z_e = 0.021$, and $d/H_P = 0.35$.

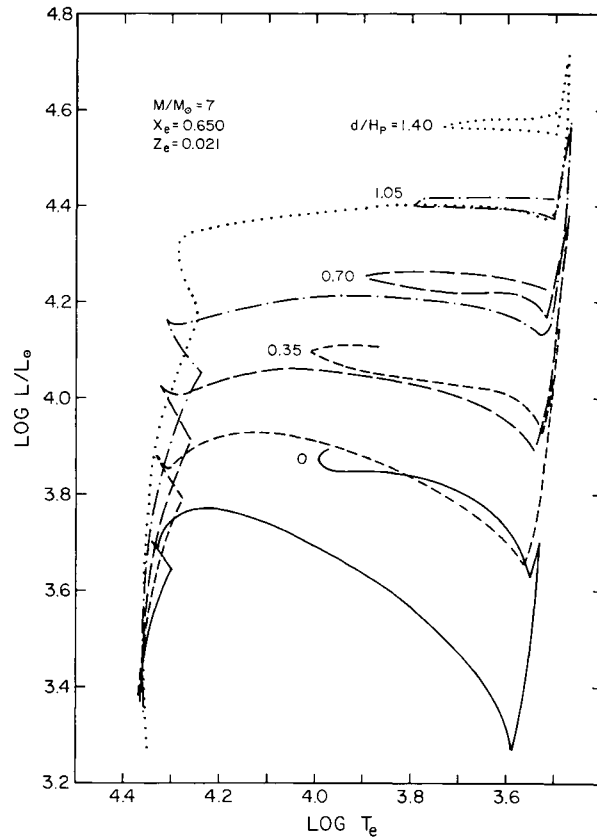


FIG. 11.—H-R diagram showing evolutionary tracks for a star of $7 M_\odot$ with $X_e = 0.650$, $Z_e = 0.021$, and various amounts of convective core overshooting, specifically $d/H_P = 0$ (case 1) and $d/H_P = 0.35, 0.70, 1.05$, and 1.40 (case 3).

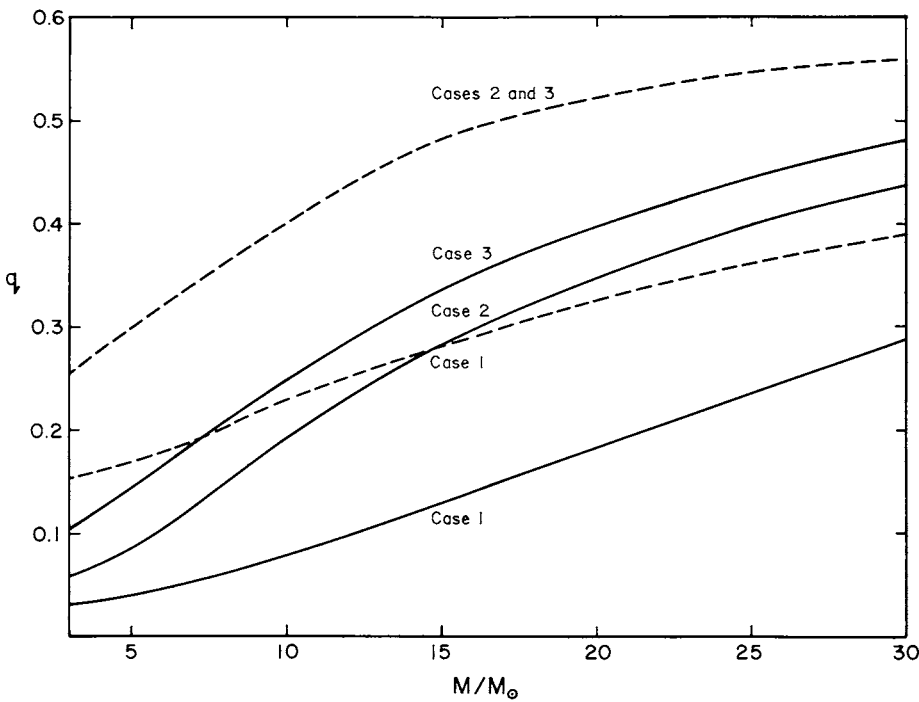


FIG. 12.—Mass fraction contained in the helium core (*dashed lines*) and in the convective central region of the core (*solid lines*) as a function of total stellar mass for cases 1, 2, and 3. The evolutionary stage shown is that at which the helium-burning convective core achieves its maximum size. Initial chemical composition of the star is $X_e = 0.739$, $Z_e = 0.021$, and convective core overshooting in cases 2 and 3 occurs with $d/H_P = 0.70$.

TABLE 1
LIFETIME OF CORE HYDROGEN BURNING AND RATIO OF LIFETIMES
OF CORE HELIUM BURNING AND CORE HYDROGEN BURNING

X_e	Z_e	M/M_\odot	$\tau_H (10^6 \text{ yr})$			τ_{He}/τ_H		
			Case 1	Case 2	Case 3	Case 1	Case 2	Case 3
0.739	0.021	3	299.633	487.141	487.141	0.330	0.039	0.056
		5	82.140	129.939	129.939	0.221	0.033	0.047
		7	40.300	61.517	61.517	0.169	0.034	0.045
		10	21.314	30.778	30.778	0.130	0.035	0.045
		15	11.921	16.210	16.210	0.094	0.040	0.044
		30	5.831	7.177	7.177	0.081	0.052	0.057
0.739	0.044	3	454.947	740.265	740.265	0.354	0.045	0.065
		5	108.113	173.361	173.361	0.257	0.035	0.053
		7	49.065	75.873	75.873	0.181	0.032	0.045
		10	24.373	35.759	35.759	0.133	0.033	0.044
		15	12.842	17.710	17.710	0.092	0.038	0.045
		30	6.172	7.511	7.511	0.076	0.049	0.054
0.650	0.021	3	185.139	300.122	300.122	0.355	0.045	0.064
		5	53.805	83.463	83.463	0.237	0.048	0.059
		7	27.401	41.102	41.102	0.187	0.042	0.056
		10	15.076	21.461	21.461	0.139	0.046	0.055
		15	8.732	11.697	11.697	0.110	0.050	0.059
		30	4.526	5.483	5.483	0.097	0.065	0.071
0.650	0.044	3	272.761	442.881	442.881	0.423	0.048	0.068
		5	68.713	108.454	108.454	0.262	0.041	0.060
		7	32.490	49.318	49.318	0.196	0.040	0.056
		10	16.841	24.333	24.333	0.147	0.044	0.054
		15	9.379	12.667	12.667	0.106	0.048	0.058
		30	5.161	5.730	5.730	0.080	0.062	0.068

NOTE.—Convective core overshooting has $d/H_P = 0.70$.

TABLE 2
RATIO OF BLUE AND RED LIFETIMES DURING CORE HELIUM DEPLETION

X_e	Z_e	M/M_\odot	τ_b/τ_r		
			Case 1	Case 2	Case 3
0.739	0.021	3	0.690	0.000	0.000
		5	<i>0.659</i>	0.000	0.546
		7	<i>0.402</i>	0.000	0.555
		10	0.592	0.000	0.000
		15	<i>0.447</i>	0.000	0.000
0.739	0.044	3	0.310	0.000	0.000
		5	<i>0.508</i>	0.000	0.000
		7	<i>0.879</i>	0.000	0.000
		10	1.595	0.000	0.000
		15	1.057	0.000	0.000
0.650	0.021	3	0.735	0.000	0.000
		5	<i>0.507</i>	0.327	0.801
		7	<i>0.489</i>	0.600	0.885
		10	0.734	0.266	0.735
		15	<i>0.608</i>	0.000	0.000
0.650	0.044	3	0.893	0.000	0.000
		5	<i>0.505</i>	0.000	0.000
		7	<i>0.946</i>	0.000	0.000
		10	1.392	0.000	0.000
		15	0.816	0.000	0.000

NOTE.—Convective core overshooting has $d/H_p = 0.70$. Italics indicate that the blue loop was artificially triggered.

TABLE 3
EFFECTIVE TEMPERATURE AND LUMINOSITY OF THE BLUE TIP DURING CORE HELIUM DEPLETION

X_e	Z_e	M/M_\odot	$\log T_e$			$\log (L/L_\odot)$		
			Case 1	Case 2	Case 3	Case 1	Case 2	Case 3
0.739	0.021	3	3.656	2.039
		5	<i>3.938</i>	...	3.773	<i>3.137</i>	...	3.526
		7	<i>4.027</i>	...	3.847	<i>3.672</i>	...	4.059
		10	4.166	4.220
		15	<i>4.237</i>	<i>4.738</i>
0.739	0.044	3	3.623	1.725
		5	<i>3.792</i>	2.811
		7	4.008	<i>3.476</i>
		10	4.125	4.050
		15	<i>4.216</i>	<i>4.639</i>
0.650	0.021	3	3.739	2.427
		5	<i>3.909</i>	3.728	3.792	3.354	3.754	3.751
		7	3.994	3.824	3.902	3.872	4.242	4.256
		10	4.179	3.763	3.873	4.406	4.682	4.693
		15	<i>4.249</i>	<i>4.894</i>
0.650	0.044	3	3.643	2.016
		5	<i>3.873</i>	<i>3.108</i>
		7	4.004	3.694
		10	4.129	4.241
		15	4.220	4.799

NOTE.—Convective core overshooting has $d/H_p = 0.70$. Italics indicate that the blue loop was artificially triggered.

TABLE 4
LUMINOSITY RANGE OF RED SUPERGIANTS
DURING CORE HELIUM DEPLETION

X_e	Z_e	M/M_\odot	log (L/L_\odot)		
			Case 1	Case 2	Case 3
0.739	0.021	3	1.896–2.064	2.462–3.003	2.460–3.029
		5	2.772–2.968	3.410–3.813	3.412–3.818
		7	3.349–3.530	3.976–4.278	3.974–4.283
		10	3.942–4.117	4.513–4.723	4.488–4.714
		15	4.545–4.720	5.003–5.143	5.001–5.146
		30	5.415–5.490	5.671–5.727	5.670–5.728
0.739	0.044	3	1.627–1.812	2.124–2.802	2.123–2.811
		5	2.496–2.787	3.073–3.662	3.074–3.669
		7	3.065–3.372	3.745–4.172	3.744–4.176
		10	3.683–4.026	4.320–4.644	4.309–4.628
		15	4.378–4.661	4.878–5.094	4.871–5.095
		30	5.315–5.461	5.611–5.713	5.606–5.714
0.650	0.021	3	2.117–2.233	2.790–3.153	2.792–3.159
		5	3.042–3.174	3.669–3.953	3.647–3.938
		7	3.628–3.707	4.171–4.394	4.172–4.378
		10	4.169–4.275	4.646–4.804	4.647–4.806
		15	4.742–4.848	5.086–5.209	5.089–5.210
		30	5.524–5.567	5.709–5.774	5.709–5.774
0.650	0.044	3	1.843–2.020	2.445–2.982	2.445–2.990
		5	2.786–2.975	3.377–3.789	3.378–3.787
		7	3.325–3.584	3.966–4.284	3.968–4.289
		10	3.934–4.188	4.497–4.730	4.495–4.734
		15	4.591–4.782	4.998–5.165	4.992–5.169
		30	5.494–5.601	5.673–5.755	5.671–5.755

NOTE.—Convective core overshooting has $d/H_P = 0.70$.

TABLE 5
CASE 3 FOR $d/H_P = 0.35$

M/M_\odot	τ_H (10^6 yr)	τ_{He}/τ_H	τ_b/τ_r	BLUE TIP		RED BRANCH log (L/L_\odot)
				log T_e	log (L/L_\odot)	
$X_e = 0.739, Z_e = 0.021$						
3	399.442	0.117	1.288	3.685	2.344	2.155–2.612
5	108.073	0.086	0.980	3.896	3.327	3.098–3.502
7	52.226	0.074	1.000	4.002	3.883	3.690–4.010
10	26.697	0.065	0.903	4.070	4.399	4.267–4.516
15	14.262	0.061	0.000	4.820–4.994
30	6.584	0.064	0.000	5.565–5.644
$X_e = 0.739, Z_e = 0.044$						
3	612.052	0.130	1.263	3.628	1.957	1.846–2.384
5	142.517	0.101	1.296	3.783	2.999	2.758–3.278
7	63.522	0.079	1.162	3.891	3.634	3.399–3.877
10	30.688	0.066	0.931	3.979	4.231	4.052–4.426
15	15.578	0.058	0.000	4.687–4.941
30	4.118	0.071	0.000	6.067–6.126
$X_e = 0.650, Z_e = 0.021$						
3	244.818	0.132	0.549	3.647	2.618	2.464–2.774
5	69.963	0.102	0.801	3.898	3.561	3.365–3.620
7	34.882	0.086	1.074	4.011	4.096	3.936–4.147
10	18.612	0.078	0.966	4.069	4.571	4.460–4.615
15	10.387	0.077	0.000	4.953–5.075
30	5.062	0.080	0.000	5.637–5.695
$X_e = 0.650, Z_e = 0.044$						
3	360.610	0.144	0.000	2.140–2.605
5	89.819	0.109	0.656	3.709	3.228	3.060–3.471
7	41.567	0.089	0.928	3.850	3.855	3.684–4.039
10	20.940	0.077	0.891	3.956	4.415	4.280–4.554
15	11.212	0.073	0.000	4.836–5.031
30	3.288	0.087	0.000	6.112–6.161

TABLE 6
THEORETICAL ZERO-AGE MAIN-SEQUENCE MODELS

M/M_{\odot}	$X_e = 0.739, Z_e = 0.021$		$X_e = 0.739, Z_e = 0.044$		$X_e = 0.650, Z_e = 0.021$		$X_e = 0.650, Z_e = 0.044$	
	$\log(L/L_{\odot})$	$\log T_e$						
$d/H_P = 0$								
3	1.875	4.106	1.661	4.035	2.059	4.147	1.856	4.079
5	2.719	4.247	2.561	4.188	2.886	4.285	2.740	4.228
7	3.230	4.330	3.109	4.279	3.386	4.365	3.275	4.317
10	3.734	4.412	3.647	4.366	3.879	4.442	3.798	4.401
15	4.262	4.492	4.203	4.454	4.391	4.520	4.336	4.486
30	5.046	4.604	5.014	4.574	5.146	4.625	5.115	4.598
$d/H_P = 0.35$								
3	1.871	4.105	1.654	4.034	2.051	4.146	1.850	4.078
5	2.713	4.246	2.556	4.187	2.882	4.284	2.736	4.227
7	3.225	4.329	3.101	4.278	3.381	4.364	3.270	4.316
10	3.733	4.409	3.644	4.366	3.875	4.442	3.794	4.401
15	4.261	4.490	4.197	4.454	4.388	4.519	4.334	4.485
30	5.044	4.601	5.011	4.574	5.144	4.625	5.113	4.598
$d/H_P = 0.70$								
3	1.855	4.103	1.632	4.030	2.030	4.143	1.841	4.076
5	2.698	4.244	2.539	4.184	2.859	4.281	2.719	4.225
7	3.208	4.327	3.084	4.275	3.369	4.363	3.255	4.314
10	3.715	4.407	3.624	4.363	3.864	4.440	3.782	4.399
15	4.245	4.488	4.185	4.452	4.374	4.518	4.318	4.484
30	5.035	4.601	5.002	4.574	5.136	4.625	5.105	4.598

TABLE 7
THEORETICAL TERMINAL-AGE MAIN-SEQUENCE MODELS

M/M_{\odot}	$X_e = 0.739, Z_e = 0.021$		$X_e = 0.739, Z_e = 0.044$		$X_e = 0.650, Z_e = 0.021$		$X_e = 0.650, Z_e = 0.044$	
	$\log(L/L_{\odot})$	$\log T_e$						
$d/H_P = 0$								
3	2.065	4.036	1.834	3.966	2.253	4.089	2.035	4.021
5	2.946	4.177	2.766	4.117	3.120	4.225	2.953	4.168
7	3.479	4.259	3.342	4.205	3.643	4.304	3.516	4.253
10	4.010	4.335	3.914	4.286	4.156	4.378	4.064	4.332
15	4.565	4.407	4.492	4.364	4.691	4.446	4.628	4.404
30	5.343	4.486	5.315	4.443	5.423	4.524	5.447	4.462
$d/H_P = 0.35$								
3	2.206	4.002	1.960	3.934	2.389	4.063	2.160	3.993
5	3.097	4.145	2.898	4.085	3.248	4.204	3.078	4.143
7	3.635	4.226	3.482	4.170	3.782	4.280	3.650	4.226
10	4.163	4.301	4.048	4.253	4.288	4.353	4.197	4.303
15	4.686	4.373	4.625	4.318	4.787	4.422	4.724	4.377
30	5.426	4.439	5.390	4.383	5.493	4.486	5.458	4.439
$d/H_P = 0.70$								
3	2.346	3.971	2.087	3.907	2.523	4.041	2.290	3.972
5	3.223	4.121	3.035	4.054	3.372	4.187	3.198	4.126
7	3.756	4.208	3.612	4.146	3.878	4.273	3.754	4.214
10	4.267	4.283	4.170	4.222	4.381	4.337	4.284	4.292
15	4.794	4.342	4.714	4.296	4.872	4.407	4.817	4.349
30	5.497	4.381	5.457	4.325	5.545	4.462	5.513	4.404

TABLE 8
 $3 M_{\odot}, X_e = 0.739, Z_e = 0.021$

t (10^6 yr)	$\log(L/L_{\odot})$	$\log T_e$	$\log T_c$	$\log \rho_c$	X_c/Y_c	q_{core}	q_{shell}	q_{env}
Case 1								
0.00	1.875	4.106	7.377	1.619	0.739	0.185
191.90	1.989	4.082	7.404	1.656	0.396	0.128
254.69	2.036	4.056	7.428	1.717	0.197	0.092
277.85	2.053	4.042	7.447	1.773	0.098	0.079
288.76	2.065	4.036	7.466	1.833	0.042	0.068
294.95	2.109	4.058	7.521	2.017	0.004	0.049
295.47	2.141	4.075	7.529	2.237	0.000	0.007
295.63	2.130	4.070	7.484	2.394	Y_c	0.000
306.62	2.192	4.022	7.520	3.326	0.979	0.000
309.93	2.076	3.842	7.817	4.193	0.979	0.000	0.100	...
310.39	1.940	3.730	7.890	4.380	0.979	0.000	0.102	...
310.79	1.660	3.621	7.955	4.548	0.979	0.000	0.103	0.853
310.95	1.802	3.595	7.980	4.613	0.979	0.000	0.103	0.483
311.70	2.064	3.587	8.053	4.526	0.976	0.024	0.106	0.200
324.61	1.925	3.595	8.063	4.424	0.902	0.024	0.121	0.432
336.70	1.906	3.599	8.071	4.388	0.804	0.025	0.127	0.531
349.48	1.897	3.603	8.081	4.353	0.705	0.028	0.135	0.635
358.40	1.896	3.608	8.089	4.340	0.607	0.029	0.139	0.713
367.34	1.906	3.616	8.097	4.334	0.495	0.030	0.143	0.799
373.62	1.926	3.624	8.105	4.334	0.409	0.030	0.145	0.867
381.07	1.981	3.640	8.117	4.343	0.297	0.030	0.149	...
386.85	2.025	3.649	8.133	4.365	0.203	0.031	0.152	...
389.60	2.039	3.656	8.142	4.381	0.156	0.031	0.154	...
392.91	2.018	3.644	8.158	4.414	0.098	0.031	0.155	...
397.99	1.972	3.605	8.220	4.591	0.001	0.028	0.157	...
Case 2								
487.57	2.239	3.618	7.793	3.529	Y_c	0.000	0.163	0.879
487.92	2.748	3.555	7.951	4.067	0.979	0.000	0.168	0.330
488.33	3.003	3.527	8.094	4.170	0.973	0.046	0.184	0.254
490.44	2.871	3.542	8.109	4.042	0.901	0.049	0.218	0.284
492.95	2.611	3.571	8.120	3.989	0.801	0.058	0.234	0.393
494.85	2.505	3.584	8.128	3.976	0.699	0.059	0.240	0.540
496.23	2.471	3.590	8.134	3.973	0.607	0.060	0.242	0.645
498.29	2.462	3.594	8.143	3.977	0.492	0.060	0.245	0.744
499.78	2.466	3.600	8.152	3.986	0.396	0.060	0.247	0.811
501.21	2.480	3.604	8.162	4.001	0.301	0.060	0.249	0.874
502.60	2.492	3.607	8.176	4.026	0.206	0.060	0.251	...
504.27	2.486	3.601	8.202	4.087	0.092	0.060	0.253	0.853
505.79	2.549	3.580	8.301	4.412	0.001	0.034	0.253	0.534
Case 3								
0.00	1.855	4.103	7.377	1.603	0.739	0.357
331.34	2.108	4.081	7.412	1.596	0.412	0.290
433.53	2.244	4.037	7.442	1.615	0.200	0.223
463.77	2.300	4.004	7.462	1.650	0.103	0.182
484.19	2.365	3.965	7.513	1.796	0.014	0.152
486.42	2.392	3.975	7.547	1.844	0.004	0.149
487.16	2.502	4.024	7.655	2.474	0.000	0.000
487.23	2.412	3.974	7.658	2.815	Y_c	0.000
487.40	2.423	3.810	7.717	3.213	0.979	0.000	0.163	...
487.52	2.310	3.657	7.768	3.435	0.979	0.000	0.163	...
487.57	2.239	3.618	7.793	3.529	0.979	0.000	0.163	0.879
487.84	2.700	3.561	7.915	3.951	0.979	0.000	0.167	0.357
488.36	3.029	3.523	8.094	4.134	0.975	0.091	0.183	0.251
491.93	2.661	3.566	8.115	3.982	0.901	0.096	0.231	0.353
495.20	2.481	3.587	8.123	3.948	0.803	0.101	0.240	0.594
497.29	2.460	3.593	8.128	3.939	0.733	0.104	0.244	0.719
500.72	2.483	3.605	8.138	3.932	0.607	0.105	0.250	0.887
503.45	2.500	3.609	8.146	3.933	0.498	0.105	0.251	...
505.58	2.509	3.610	8.155	3.938	0.407	0.105	0.253	...
507.99	2.517	3.610	8.168	3.951	0.298	0.105	0.254	...
509.89	2.515	3.607	8.181	3.972	0.207	0.104	0.256	...
512.12	2.507	3.601	8.201	4.023	0.099	0.102	0.257	0.859
514.35	2.584	3.577	8.319	4.361	0.001	0.085	0.258	0.520

NOTE.—Convective core overshooting has $d/H_P = 0.70$.

TABLE 9
 $5 M_{\odot}$, $X_e = 0.739$, $Z_e = 0.021$

t (10^6 yr)	$\log(L/L_{\odot})$	$\log T_e$	$\log T_c$	$\log \rho_c$	X_c/Y_c	q_{core}	q_{shell}	q_{env}
Case 1								
0.00	2.719	4.247	7.429	1.331	0.739	0.230
52.65	2.847	4.224	7.458	1.353	0.407	0.157
70.03	2.904	4.199	7.482	1.407	0.208	0.118
76.27	2.927	4.185	7.500	1.459	0.109	0.100
79.95	2.946	4.177	7.526	1.538	0.038	0.086
81.60	3.006	4.212	7.598	1.944	0.000	0.012
81.64	2.994	4.207	7.554	2.122	0.000	0.000
83.50	3.058	4.144	7.608	3.121	Y_c	0.000
84.13	2.955	3.930	7.920	3.962	0.979	0.000	0.113	...
84.22	2.803	3.771	7.986	4.127	0.979	0.000	0.114	...
84.25	2.655	3.670	8.010	4.186	0.979	0.000	0.115	...
84.28	2.518	3.613	8.032	4.273	0.979	0.000	0.115	0.810
84.30	2.745	3.586	8.048	4.266	0.979	0.000	0.115	0.384
84.46	2.968	3.566	8.100	4.125	0.973	0.031	0.118	0.182
86.53	2.912	3.572	8.110	4.031	0.901	0.032	0.134	0.264
88.89	2.860	3.578	8.121	3.980	0.801	0.034	0.144	0.379
90.65	2.814	3.584	8.130	3.958	0.702	0.037	0.150	0.509
92.25	2.782	3.591	8.139	3.948	0.601	0.038	0.154	0.656
93.03	2.772	3.595	8.143	3.947	0.549	0.038	0.156	0.720
93.82	2.789	3.604	8.148	3.947	0.493	0.039	0.158	0.810
94.66	2.980	3.745	8.154	3.954	0.432	0.039	0.160	...
95.13	3.018	3.813	8.157	3.956	0.398	0.039	0.162	...
96.75	3.085	3.896	8.171	3.947	0.306	0.041	0.168	...
97.96	3.113	3.924	8.186	3.963	0.202	0.042	0.173	...
99.28	3.137	3.938	8.217	4.020	0.083	0.043	0.179	...
100.29	3.050	3.792	8.302	4.288	0.002	0.023	0.182	...
Case 2								
130.05	3.140	3.586	7.917	3.285	Y_c	0.000	0.201	...
130.06	3.360	3.541	7.936	3.348	0.979	0.000	0.203	0.583
130.18	3.813	3.487	8.147	3.736	0.971	0.064	0.222	0.306
130.61	3.727	3.497	8.159	3.637	0.901	0.071	0.255	0.331
131.13	3.601	3.512	8.168	3.597	0.801	0.078	0.271	0.374
131.57	3.510	3.525	8.177	3.583	0.697	0.081	0.279	0.445
131.93	3.452	3.534	8.185	3.581	0.607	0.082	0.284	0.536
132.34	3.422	3.539	8.194	3.587	0.497	0.084	0.288	0.634
132.72	3.412	3.545	8.204	3.600	0.392	0.084	0.292	0.722
133.03	3.410	3.549	8.215	3.617	0.306	0.084	0.294	0.794
133.40	3.415	3.552	8.230	3.650	0.202	0.085	0.296	0.837
133.79	3.424	3.551	8.255	3.711	0.097	0.084	0.298	0.826
134.22	3.488	3.530	8.352	4.031	0.001	0.042	0.301	0.541
Case 3								
0.00	2.698	4.244	7.428	1.315	0.739	0.392
88.24	2.950	4.223	7.465	1.292	0.409	0.318
115.38	3.115	4.183	7.497	1.331	0.200	0.262
123.43	3.178	4.151	7.517	1.369	0.106	0.236
129.18	3.250	4.111	7.570	1.504	0.015	0.197
129.81	3.273	4.123	7.608	1.612	0.003	0.189
129.95	3.366	4.167	7.741	2.227	0.000	0.000
129.97	3.307	4.119	7.765	2.572	0.000	0.000
130.00	3.336	3.984	7.822	2.909	Y_c	0.000
130.03	3.293	3.785	7.879	3.147	0.979	0.000	0.201	...
130.05	3.140	3.586	7.917	3.285	0.979	0.000	0.201	...
130.06	3.410	3.535	7.940	3.361	0.979	0.000	0.203	0.521
130.18	3.818	3.487	8.147	3.722	0.975	0.108	0.222	0.306
130.92	3.652	3.506	8.163	3.589	0.902	0.127	0.267	0.353
131.68	3.491	3.528	8.173	3.553	0.798	0.133	0.282	0.474
132.41	3.424	3.539	8.182	3.540	0.694	0.137	0.289	0.642
132.83	3.412	3.546	8.187	3.534	0.623	0.139	0.293	0.754
133.50	3.479	3.613	8.200	3.538	0.501	0.142	0.299	...
133.56	3.485	3.643	8.201	3.539	0.490	0.142	0.299	...
134.01	3.514	3.744	8.209	3.545	0.403	0.144	0.306	...
134.46	3.526	3.773	8.220	3.558	0.312	0.145	0.307	...
134.98	3.526	3.743	8.237	3.588	0.204	0.145	0.309	...
135.50	3.513	3.655	8.263	3.646	0.098	0.145	0.310	...
136.06	3.516	3.529	8.380	3.989	0.001	0.115	0.311	...

NOTE.—Convective core overshooting has $d/H_P = 0.70$.

TABLE 10
 $7 M_{\odot}, X_e = 0.739, Z_e = 0.021$

t (10^6 yr)	$\log(L/L_{\odot})$	$\log T_e$	$\log T_c$	$\log \rho_c$	X_c/Y_c	q_{core}	q_{shell}	q_{env}
Case 1								
0.000	3.230	4.330	7.461	1.147	0.739	0.267
26.190	3.371	4.306	7.491	1.167	0.399	0.181
34.618	3.435	4.281	7.516	1.220	0.201	0.139
37.785	3.462	4.266	7.535	1.273	0.102	0.119
39.484	3.484	4.258	7.563	1.359	0.034	0.105
40.163	3.511	4.275	7.615	1.522	0.004	0.088
40.251	3.541	4.294	7.654	1.775	0.000	0.024
40.270	3.523	4.286	7.614	2.022	Y_c	0.000
40.629	3.584	4.201	7.715	3.054	0.979	0.000
40.785	3.539	4.056	7.932	3.644	0.979	0.000	0.122	...
40.837	3.430	3.884	8.027	3.878	0.979	0.000	0.126	...
40.855	3.309	3.751	8.060	3.955	0.979	0.000	0.127	...
40.869	3.054	3.596	8.096	3.997	0.978	0.002	0.127	0.880
40.873	3.231	3.568	8.108	4.000	0.978	0.006	0.127	0.499
40.934	3.530	3.537	8.131	3.851	0.972	0.035	0.130	0.201
41.707	3.485	3.543	8.143	3.757	0.901	0.040	0.148	0.259
42.516	3.455	3.546	8.153	3.716	0.804	0.042	0.158	0.317
43.355	3.416	3.552	8.164	3.687	0.701	0.047	0.167	0.420
43.981	3.385	3.556	8.172	3.678	0.599	0.048	0.172	0.528
44.517	3.364	3.561	8.180	3.677	0.504	0.049	0.175	0.625
45.118	3.349	3.567	8.192	3.684	0.390	0.049	0.178	0.781
45.357	3.506	3.658	8.199	3.695	0.343	0.049	0.180	...
45.389	3.589	3.809	8.200	3.698	0.337	0.049	0.180	...
45.554	3.610	3.940	8.202	3.705	0.305	0.049	0.181	...
46.103	3.646	3.996	8.221	3.726	0.193	0.051	0.187	...
46.620	3.672	4.027	8.255	3.795	0.087	0.051	0.195	...
46.963	3.672	4.011	8.292	3.891	0.022	0.051	0.198	...
47.091	3.644	3.947	8.338	4.081	0.001	0.019	0.200	...
Case 2								
61.575	4.109	3.487	8.059	3.307	Y_c	0.000	0.242	0.429
61.614	4.278	3.472	8.182	3.450	0.969	0.081	0.258	0.353
61.793	4.217	3.478	8.191	3.380	0.901	0.094	0.288	0.373
62.037	4.130	3.487	8.202	3.348	0.800	0.106	0.308	0.406
62.230	4.070	3.494	8.210	3.339	0.703	0.111	0.317	0.448
62.431	4.025	3.502	8.218	3.341	0.594	0.113	0.323	0.509
62.608	3.998	3.506	8.227	3.349	0.495	0.115	0.327	0.573
62.829	3.980	3.512	8.239	3.358	0.401	0.123	0.332	0.678
62.996	3.976	3.516	8.250	3.378	0.304	0.124	0.335	0.741
63.167	3.977	3.518	8.266	3.414	0.205	0.125	0.338	0.768
63.363	3.983	3.516	8.292	3.477	0.099	0.125	0.340	0.751
63.582	4.072	3.496	8.404	3.821	0.001	0.081	0.342	0.487
Case 3								
0.000	3.208	4.327	7.460	1.133	0.739	0.429
42.403	3.482	4.309	7.498	1.116	0.399	0.359
54.154	3.627	4.273	7.527	1.138	0.209	0.303
58.746	3.714	4.234	7.553	1.189	0.095	0.265
61.082	3.786	4.193	7.600	1.318	0.017	0.239
61.520	3.891	4.246	7.794	2.028	0.000	0.000
61.532	3.847	4.197	7.844	2.431	0.000	0.000
61.544	3.867	4.076	7.899	2.719	Y_c	0.000
61.555	3.858	3.897	7.953	2.938	0.979	0.000	0.237	...
61.561	3.795	3.671	7.988	3.066	0.979	0.000	0.238	...
61.564	3.703	3.547	8.004	3.124	0.979	0.000	0.239	0.876
61.575	4.109	3.487	8.059	3.307	0.979	0.000	0.242	0.429
61.611	4.283	3.471	8.182	3.441	0.974	0.128	0.258	0.351
61.911	4.176	3.481	8.194	3.344	0.900	0.152	0.300	0.384
62.265	4.075	3.494	8.203	3.315	0.806	0.160	0.317	0.441
62.528	4.004	3.505	8.213	3.308	0.701	0.171	0.326	0.549
62.809	3.976	3.513	8.221	3.305	0.602	0.174	0.332	0.679
63.041	3.974	3.521	8.230	3.312	0.507	0.179	0.337	0.815
63.233	4.028	3.671	8.240	3.324	0.425	0.180	0.340	...
63.286	4.033	3.721	8.242	3.326	0.402	0.181	0.340	...
63.568	4.051	3.817	8.257	3.351	0.296	0.185	0.345	...
63.775	4.059	3.847	8.271	3.371	0.205	0.185	0.349	...
64.019	4.058	3.799	8.297	3.433	0.098	0.186	0.353	...
64.139	4.044	3.689	8.325	3.506	0.051	0.185	0.353	...
64.288	4.049	3.502	8.413	3.786	0.001	0.168	0.355	...

NOTE.—Convective core overshooting has $d/H_p = 0.70$.

TABLE 11
 $10 M_{\odot}, X_e = 0.739, Z_e = 0.021$

t (10^6 yr)	$\log (L/L_{\odot})$	$\log T_e$	$\log T_c$	$\log \rho_c$	X_c/Y_c	q_{core}	q_{shell}	q_{env}
Case 1								
0.000	3.734	4.412	7.492	0.967	0.739	0.315
13.891	3.887	4.386	7.523	0.984	0.397	0.220
18.380	3.960	4.360	7.549	1.038	0.199	0.174
20.001	3.991	4.344	7.569	1.094	0.101	0.153
20.923	4.015	4.334	7.597	1.182	0.033	0.134
21.262	4.039	4.350	7.650	1.346	0.004	0.118
21.312	4.070	4.371	7.712	1.661	0.000	0.030
21.321	4.049	4.359	7.698	1.929	0.000	0.000
21.393	4.104	4.255	7.830	2.871	Y_c	0.000
21.445	4.065	4.055	8.042	3.482	0.979	0.000	0.145	...
21.460	3.952	3.872	8.120	3.654	0.978	0.000	0.145	...
21.465	3.833	3.712	8.154	3.666	0.977	0.014	0.149	...
21.468	3.638	3.568	8.165	3.644	0.976	0.025	0.150	0.889
21.469	3.807	3.539	8.166	3.634	0.976	0.028	0.150	0.493
21.496	4.117	3.506	8.168	3.531	0.969	0.047	0.154	0.231
21.756	4.097	3.509	8.179	3.462	0.900	0.053	0.173	0.252
22.088	4.055	3.515	8.190	3.421	0.801	0.060	0.187	0.283
22.391	4.017	3.519	8.201	3.402	0.702	0.066	0.196	0.334
22.644	3.982	3.524	8.210	3.399	0.597	0.068	0.202	0.423
22.860	3.955	3.529	8.219	3.403	0.502	0.070	0.205	0.549
23.060	3.942	3.538	8.227	3.404	0.434	0.073	0.209	0.773
23.120	4.075	3.626	8.231	3.410	0.406	0.073	0.210	...
23.130	4.165	3.829	8.231	3.411	0.401	0.073	0.210	...
23.138	4.187	3.933	8.231	3.413	0.398	0.073	0.210	...
23.149	4.185	4.020	8.231	3.415	0.392	0.073	0.210	...
23.350	4.185	4.102	8.240	3.426	0.317	0.073	0.215	...
23.535	4.204	4.140	8.260	3.457	0.207	0.076	0.221	...
23.815	4.220	4.166	8.284	3.496	0.113	0.080	0.230	...
24.042	4.215	4.113	8.350	3.674	0.014	0.077	0.232	...
24.068	4.204	4.081	8.377	3.759	0.005	0.069	0.233	...
Case 2								
30.805	4.505	3.484	8.114	3.018	Y_c	0.000	0.293	0.509
30.822	4.723	3.472	8.217	3.177	0.969	0.114	0.312	0.416
30.907	4.671	3.473	8.225	3.133	0.901	0.141	0.342	0.433
31.017	4.631	3.475	8.233	3.117	0.802	0.153	0.357	0.449
31.130	4.576	3.479	8.243	3.114	0.698	0.165	0.370	0.485
31.234	4.544	3.483	8.251	3.117	0.603	0.173	0.378	0.525
31.335	4.527	3.486	8.261	3.129	0.496	0.177	0.383	0.563
31.428	4.519	3.488	8.271	3.147	0.396	0.180	0.386	0.590
31.534	4.514	3.489	8.283	3.168	0.305	0.186	0.388	0.616
31.642	4.513	3.490	8.302	3.212	0.192	0.189	0.393	0.631
31.739	4.521	3.489	8.326	3.275	0.099	0.190	0.395	0.611
31.862	4.623	3.477	8.446	3.631	0.001	0.154	0.397	0.474
Case 3								
0.000	3.715	4.407	7.492	0.954	0.739	0.481
20.754	3.984	4.391	7.529	0.940	0.405	0.405
26.980	4.146	4.351	7.560	0.977	0.206	0.353
29.084	4.221	4.314	7.582	1.023	0.107	0.322
30.591	4.299	4.266	7.638	1.174	0.014	0.287
30.719	4.313	4.273	7.669	1.264	0.004	0.280
30.781	4.393	4.318	7.866	1.932	0.000	0.000
30.792	4.368	4.217	7.964	2.436	Y_c	0.000
30.794	4.370	4.177	7.985	2.532	0.979	0.000
30.799	4.367	4.019	8.041	2.761	0.979	0.000	0.290	...
30.802	4.339	3.822	8.078	2.894	0.979	0.000	0.291	...
30.804	4.294	3.658	8.094	2.951	0.979	0.000	0.291	...
30.804	4.202	3.524	8.105	2.987	0.979	0.000	0.292	0.876
30.805	4.406	3.493	8.110	3.006	0.979	0.000	0.292	0.563
30.829	4.714	3.471	8.215	3.154	0.970	0.205	0.310	0.409
30.962	4.640	3.474	8.226	3.115	0.900	0.205	0.346	0.432
31.117	4.571	3.478	8.236	3.103	0.800	0.220	0.363	0.470
31.259	4.526	3.485	8.244	3.099	0.699	0.224	0.369	0.528
31.398	4.503	3.489	8.252	3.103	0.597	0.231	0.378	0.583
31.530	4.491	3.493	8.262	3.114	0.497	0.238	0.384	0.645
31.652	4.488	3.495	8.273	3.132	0.395	0.240	0.387	0.695
31.780	4.489	3.496	8.287	3.156	0.294	0.242	0.390	0.713
31.890	4.493	3.495	8.303	3.194	0.201	0.245	0.391	0.687
32.018	4.506	3.491	8.332	3.267	0.101	0.246	0.393	0.619
32.156	4.563	3.481	8.410	3.490	0.009	0.242	0.394	0.509

NOTE.—Convective core overshooting has $d/H_P = 0.70$.

TABLE 13
 $30 M_{\odot}, X_e = 0.739, Z_e = 0.021$

t (10^6 yr)	$\log(L/L_{\odot})$	$\log T_e$	$\log T_c$	$\log \rho_c$	X_c/Y_c	q_{core}	q_{shell}	q_{env}
Case 1								
0.000	5.046	4.604	7.570	0.526	0.739	0.546
3.568	5.202	4.576	7.598	0.550	0.410	0.439
4.908	5.286	4.536	7.624	0.608	0.205	0.363
5.454	5.325	4.503	7.647	0.675	0.094	0.327
5.767	5.354	4.480	7.692	0.814	0.017	0.298
5.815	5.364	4.489	7.732	0.935	0.004	0.286
5.831	5.393	4.526	7.875	1.401	0.000	0.161
5.836	5.412	4.432	8.026	2.000	Y_c	0.017
5.840	5.422	4.318	8.138	2.397	0.979	0.000	0.299	...
5.843	5.419	4.186	8.241	2.723	0.978	0.041	0.301	...
5.846	5.395	3.995	8.275	2.794	0.972	0.151	0.302	...
5.847	5.370	3.812	8.276	2.788	0.969	0.170	0.305	...
5.847	5.328	3.671	8.276	2.786	0.968	0.174	0.306	...
5.848	5.220	3.532	8.276	2.785	0.968	0.178	0.306	...
5.848	5.386	3.497	8.276	2.785	0.967	0.178	0.306	0.477
5.857	5.490	3.493	8.279	2.774	0.944	0.195	0.316	0.404
5.877	5.482	3.496	8.281	2.766	0.897	0.206	0.326	0.404
5.918	5.467	3.497	8.289	2.765	0.805	0.225	0.343	0.404
5.964	5.451	3.496	8.296	2.769	0.701	0.236	0.353	0.407
6.005	5.439	3.495	8.303	2.779	0.607	0.236	0.361	0.410
6.052	5.426	3.494	8.314	2.799	0.497	0.245	0.366	0.416
6.096	5.418	3.494	8.325	2.825	0.397	0.263	0.371	0.420
6.127	5.415	3.494	8.335	2.844	0.322	0.266	0.373	0.422
6.187	5.421	3.494	8.356	2.897	0.197	0.272	0.375	0.420
6.245	5.435	3.495	8.383	2.971	0.092	0.276	0.376	0.412
6.283	5.468	3.498	8.441	3.138	0.019	0.273	0.379	0.408
Case 2								
7.182	5.560	4.193	8.201	2.356	Y_c	0.000
7.184	5.549	3.922	8.262	2.550	0.979	0.229	0.499	...
7.184	5.542	3.812	8.272	2.581	0.978	0.247	0.499	...
7.184	5.524	3.679	8.280	2.605	0.978	0.262	0.499	...
7.185	5.448	3.527	8.284	2.619	0.978	0.276	0.499	...
7.185	5.609	3.504	8.287	2.628	0.977	0.282	0.499	0.659
7.188	5.727	3.508	8.296	2.648	0.968	0.350	0.501	0.600
7.210	5.711	3.508	8.300	2.646	0.900	0.374	0.518	0.600
7.245	5.691	3.506	8.307	2.654	0.793	0.395	0.533	0.600
7.277	5.681	3.506	8.314	2.668	0.694	0.404	0.542	0.600
7.310	5.675	3.506	8.322	2.680	0.600	0.414	0.546	0.602
7.340	5.671	3.507	8.330	2.699	0.505	0.420	0.550	0.603
7.378	5.671	3.507	8.341	2.724	0.403	0.429	0.553	0.603
7.411	5.675	3.507	8.352	2.755	0.309	0.432	0.555	0.602
7.453	5.683	3.506	8.372	2.807	0.196	0.436	0.557	0.601
7.508	5.691	3.506	8.387	2.848	0.076	0.440	0.558	0.600
7.546	5.748	3.509	8.531	3.276	0.001	0.411	0.560	0.599
Case 3								
0.000	5.035	4.601	7.569	0.522	0.739	0.669
4.541	5.260	4.579	7.602	0.537	0.401	0.609
6.103	5.387	4.524	7.630	0.584	0.203	0.555
6.684	5.449	4.464	7.651	0.639	0.104	0.524
7.114	5.518	4.331	7.706	0.806	0.015	0.493
7.157	5.529	4.308	7.738	0.903	0.005	0.485
7.179	5.570	4.343	8.079	1.954	0.000	0.000
7.182	5.560	4.193	8.201	2.356	Y_c	0.000
7.183	5.556	4.080	8.235	2.463	0.979	0.322	0.499	...
7.184	5.544	3.838	8.269	2.573	0.979	0.322	0.499	...
7.184	5.531	3.715	8.278	2.598	0.978	0.338	0.499	...
7.185	5.453	3.532	8.284	2.616	0.978	0.350	0.499	...
7.185	5.550	3.505	8.285	2.621	0.978	0.350	0.499	0.687
7.188	5.728	3.507	8.295	2.645	0.969	0.404	0.501	0.600
7.214	5.708	3.508	8.300	2.643	0.899	0.428	0.522	0.599
7.249	5.691	3.507	8.306	2.648	0.804	0.441	0.535	0.599
7.291	5.677	3.506	8.315	2.662	0.693	0.456	0.543	0.601
7.328	5.671	3.506	8.322	2.676	0.593	0.461	0.550	0.603
7.363	5.670	3.506	8.331	2.696	0.498	0.470	0.553	0.603
7.403	5.671	3.506	8.340	2.716	0.399	0.470	0.556	0.603
7.439	5.676	3.506	8.353	2.751	0.304	0.477	0.558	0.602
7.485	5.688	3.507	8.373	2.804	0.192	0.481	0.560	0.600
7.530	5.702	3.508	8.400	2.878	0.097	0.483	0.561	0.599
7.581	5.755	3.510	8.535	3.281	0.001	0.447	0.562	0.590

NOTE.—Convective core overshooting has $d/H_p = 0.70$.

TABLE 14
SUPPLEMENTARY RATIOS OF BLUE AND RED LIFETIMES DURING CORE HELIUM DEPLETION

M_i/M_\odot	X_e	Z_e	d/H_P	α_P	θ_a^2	MASS LOSS	FINAL M/M_\odot	τ_{He}/τ_H	τ_b/τ_r	BLUE TIP	
										$\log T_e$	$\log (L/L_\odot)$
7	0.650	0.021	0.70	1	0.1	No	7	0.056	0.885	3.902	4.256
				2	0.1	No	7	0.056	2.446	3.867	4.261
10	0.739	0.021	0.00	1	0.1	No	10	0.130	0.592	4.166	4.220
				1	0.1	Yes	9.7	0.128	0.902	4.157	4.194
15	0.650	0.021	0.35	1	0.1	No	15	0.077	0.000
				2	0.1	No	15	0.077	0.444	3.965	5.003
				1	1.0	No	15	0.086	0.490	4.059	5.008
15	0.650	0.044	0.35	1	0.1	No	15	0.073	0.000
				2	0.1	No	15	0.074	0.647	4.012	4.919

NOTE.—Convective core overshooting refers to case 3.

TABLE 15

EVOLUTIONARY SEQUENCES OF INTERMEDIATE-MASS AND HIGH-MASS STARS WITH CONVECTIVE CORE OVERSHOOTING PUBLISHED BY OTHER AUTHORS

Author and Date	X_e	Z_e	d/H_P	M_i/M_\odot	N	Remarks
Maeder 1976	0.700	0.030	$\lesssim 0.17$	3	3	MS mainly
Massevitch et al. 1979	0.602	0.044	$\lesssim \text{Large}$	10, 16, 32, 64, 128	0	MS only
Cloutman & Whitaker 1980	0.700	0.020	~ 0.7	15.57	0	
Maeder & Mermilliod 1981	0.700	0.030	$\lesssim 0.17$	5, 9	6	MS mainly
Bressan, Bertelli, & Chiosi 1981	0.700	0.020	~ 0.35	20, 60, 100	0	MS only; mass loss
Matraka, Wassermann, & Weigert 1982	0.602	0.044	$\lesssim 0.17$	4, 5, 6, 7, 8	10	
Becker & Cox 1982	0.690	0.030	~ 0.3	9	0	
Maeder 1982	0.700	0.030	0.15+	30, 60	0	MS only; mass loss
de Loore 1982	0.700	0.030	Moderate	40, 60, 100	0	MS only; mass loss
Doom 1982a, b	0.700	0.030	≤ 1.7	10, 15, 20, 30, 35, 40, 60, 80, 100	9	MS only; mass loss
Huang & Weigert 1983	0.602	0.044	$\lesssim 0.17$	5	0	
Bertelli, Bressan, & Chiosi 1984	0.700	0.020	$\lesssim 0.7$	20	0	Mass loss
Bertelli, Bressan, & Chiosi 1985	0.700	0.020	$\lesssim 0.35$	3, 4, 5, 6, 7, 9	0	Mass loss
Doom 1985	0.700	0.030	~ 2	3, 4, 5, 6, 7, 8, 10, 15, 20, 30, 40, 60, 100, 120	0	MS mainly; mass loss
Polyser, Doom, & de Loore 1985	0.700	0.030	~ 2	28–36	0	MS only; mass loss
Xiong 1985, 1986	0.700	0.030	$\lesssim 2$	7, 15, 30, 60	8	MS only
Doom, De Grève, & de Loore 1986 ...	0.700	0.030	~ 2	15–180	0	Mass loss
Prantzos et al. 1986	0.700	0.030	~ 2	40, 50, 60, 80, 100	0	Mass loss
Bertelli et al. 1986, 1990	0.700	0.001	~ 0.35	3, 4, 4.5, 5, 6, 7, 9	7	
	0.750	0.004	~ 0.35	3, 4, 4.5, 5, 6, 7, 9	0	
	0.700	0.020	~ 0.35	3, 4, 4.5, 5, 6, 7, 9	6	
Langer & El Eid 1986	0.700	0.030	1.9	100	2	Mass loss
Cloutman 1987	0.700	0.020	~ 1.8	15.57	0	MS only
Maeder & Meynet 1987	0.700	0.020	0.25	15, 20, 25, 40, 60, 85, 120	7	Mass loss
Staritsin 1988	0.750	0.020	$\lesssim \text{Large}$	4, 8	1	MS mainly; mass loss
Maeder & Meynet 1988, 1989	0.700	0.020	0.25	3, 4, 5, 7, 9, 12, 15, 20, 25, 40, 60, 85, 120	13	Mass loss
Langer, Arcoragi, & Arnould 1989	0.700	0.030	0.4	30	1	Mass loss
Maeder 1990	0.754	0.002	0.25	15, 20, 25, 40, 60, 85, 120	7	Mass loss
	0.745	0.005	0.25	15, 20, 25, 40, 60, 85, 120	7	Mass loss
	0.700	0.020	0.25	15, 20, 25, 40, 60, 85, 120	7	Mass loss
	0.640	0.040	0.25	15, 20, 25, 40, 60, 85, 120	7	Mass loss

NOTE.— N is the number of evolutionary sequences calculated with and without convective core overshooting and published in tabular form. “MS” stands for “main sequence.”